

# ANALYSIS OF RIGOROUS ORIENTATION MODELS FOR PUSHBROOM SENSORS. APPLICATIONS WITH QUICKBIRD

M. Crespi,<sup>a</sup>, F. Giannone<sup>\*a</sup>, D. Poli<sup>b</sup>

<sup>a</sup> DITS - Area di Geodesia e Geomatica, Università di Roma "La Sapienza", via Eudossiana 18, 00184 Rome, Italy - (mattia.crespi, francesca.giannone)@uniroma1.it

<sup>b</sup> CyberCity AG, Schaffhauserstrasse 481, 8052 Zurich, Switzerland - dpoli@cybercity.tv

## Commission I, WG V

**KEY WORDS:** Pushbroom, Orientation, Modelling, Bundle adjustment, QuickBird

### ABSTRACT:

The correct georeferencing of remote sensing images is a fundamental task in the photogrammetric processing for orthoimages and DEM generation and for feature extraction. In this paper we focus on the georeferencing of pushbroom sensors with rigorous models, that is, approaches that are based on the photogrammetric collinearity equations and describe the exact acquisition geometry of the sensors. By solving a bundle adjustment, the sensor external orientation and additional geometric parameters describing the internal orientation are estimated. We tested two rigorous models developed in academic groups for the georeferencing of a stereopair from QuickBird. The first model (M1) has been implemented at the University La Sapienza, Rome. It is specifically designed for the orthorectification of pushbroom sensors carried on satellite platforms with asynchronous acquisition mode, like EROS-A and QuickBird. The model, implemented in the software SISAR, reconstructs of the orbital segment during the image acquisition through the knowledge of Keplerian orbital parameters, the sensor attitude, internal orientation and the self-calibration parameters. The second model (M2) is a rigorous sensor model for pushbroom linear array sensors, carried on airborne or spaceborne platforms. It estimates the parameters modelling the sensor internal and external orientation through a bundle adjustment, using a suitable number of ground control points. Our research included the orientation of the single images with rigorous model M1, the orientation of the stereo pair with rigorous model M2 and the comparison of the results with a rigorous model contained in commercial software (PCI OrthoEngine). The results demonstrate that by using rigorous models it is possible to achieve RMSE smaller than 1 pixel in the CPs if a sufficient number of GCPs are used.

## 1. INTRODUCTION

The correct georeferencing of remote sensing images is a fundamental task in the photogrammetric processing for orthoimages and DEM generation and for 2D/3D feature extraction. In particular the georeferencing of high-resolution sensors receive a great attention, thanks to their large potential for topographic, cartographic and remote sensing applications. Most of the high-resolution satellites use linear CCD arrays that scan the Earth surface in a pushbroom mode; in most cases they can also produce stereo images across- or along- the flight direction. The main advantage of along-track stereo geometry with respect to the across-track one is that the time delay between the stereo images acquisition is smaller, resulting in small illumination and coverage differences. The along-track acquisition can be synchronous, if the satellite ground speed and the rate of imaging are equal, or asynchronous, if the satellite ground speed is faster than the rate of imaging.

In order to georeference images from pushbroom sensors different approaches are followed in the photogrammetric community. In particular in this paper we focus on rigorous models, which are based on the photogrammetric collinearity equations and describe the exact acquisition geometry of the sensors. By solving a bundle adjustment, the sensor external orientation and additional geometric parameters describing the internal orientation are estimated (Ebner et al., 1992; Kornus, 1998; Kratky, 1989). The models that can be found in literature differ for the approach followed for the description of the internal and external orientation. The rigorous modeling has the

advantage of allowing the analysis of each single internal and external orientation parameter and to study their physical behavior. For this reason it is very important to reconstruct the orbital segment during the image acquisition through the knowledge of the acquisition mode, the sensor features and the satellite position and attitude model. In addition, the effects of systematic errors in the optical systems should be taken into account. The need of a detailed description of the system brings the disadvantage that rigorous models are usually quite complex to develop.

In this paper two rigorous models developed in academic groups are used to orient a stereo pair from QuickBird acquired over Augusta (Sicily), in Italy. The first model (M1) has been implemented at the University of Rome "La Sapienza", by the Geodesy and Geomatics Team (DITS Department) and will be used for the orientation of single images; the second one (M2), developed at ETH Zurich, Institute for Geodesy and Photogrammetry, will be used for the simultaneous georeferencing of the two stereo images.

After presenting the models, the achieved results are shown and commented.

## 2. RIGOROUS MODEL IN SOFTWARE SISAR (M1)

### 2.1 Model parametrization

Since 2003, the research group of the Geodesy and Geomatics Team has developed a specific and rigorous model designed for the orientation of imagery acquired by pushbroom sensors

---

\* Corresponding author.

carried on satellite platforms with asynchronous acquisition mode, like EROS-A and QuickBird.

The first version of the model (Crespi et al., 2003) was uniquely focused on EROS-A imagery, since no commercial software including a rigorous model for this platform were available at that time. Later, the model was refined (Baiocchi et al., 2004) and extended to process QuickBird imagery too.

The model, implemented in the software SISAR, bases the indirect orientation of the imagery on the well known collinearity equations, including different subsets of parameters (Table 1) for the satellite position, the sensor attitude and the viewing geometry (internal orientation and self-calibration). In particular, the satellite position is described through the Keplerian orbital parameters attaining to the orbital segment during the image acquisition; the sensor attitude is supposed to be represented by a known time-dependent term plus a 2<sup>nd</sup> order time-dependent polynomial, one for each attitude angle; moreover, atmospheric refraction is accounted for by a general model for remote sensing applications (Noerdlinger, 1999).

SATELLITE POSITION	a: semi-major axis e: eccentricity $\Omega$ : right ascension of the ascending node i: orbit inclination $\omega$ : argument of the perigee v: true anomaly (dependent on $T_p$ , the time of the passage at perigee)
SENSOR ATTITUDE	$\phi = \phi_0(t) + a_0 + a_1 t + a_2 t^2$ (roll) $\theta = \theta_0(t) + b_0 + b_1 t + b_2 t^2$ (pitch) $\psi = \psi_0(t) + c_0 + c_1 t + c_2 t^2$ (yaw)
VIEWING GEOMETRY	f: focal length $d_1, d_2$ : self-calibration parameters

Table 1. Full parametrization of the SISAR model

In order to relate the image to the ground coordinates (expressed in an ECEF reference frame, usually a realization of WGS84, e.g. ITRF2000) by the collinearity equations, a set of rotation matrices (for details see Crespi et al., 2003; Baiocchi et al., 2004; Fratarcangeli F., 2006) involving the following coordinate systems have to be used:

- Sensor coordinate system (S) - the origin is located at the perspective center (satellite's center of mass), the  $x_S$ -axis points to the direction of satellite motion,  $z_S$ -axis is directed from the array towards the perspective center, while  $y_S$ -axis is parallel to the array of detectors, completing a right-handed system
- Satellite coordinate system (B) - the origin is located at the perspective center (satellite's center of mass) and the  $x_B$ ,  $y_B$  e  $z_B$  axes coincide with the Orbital coordinate system (F) (see below) axes when the attitude angles ( $\phi$ ,  $\theta$ ,  $\psi$ ) are zero. The  $R_{SB}$  (*Body-Sensor*) matrix gives the transformation between the B-system and the S-system. It considers the non-parallelism between the axes ( $x$ ,  $y$ ,  $z$ )<sub>S</sub> and ( $x$ ,  $y$ ,  $z$ )<sub>B</sub> and is constant within one scene for each particular sensor; the matrix elements are provided by metadata files
- Orbital coordinate system (F) - the origin is located at the satellite's center of mass, the  $x_F$ -axis is tangent to the orbit in the same direction of satellite motion, the  $z_F$ -axis is in the orbital plane like the  $x_F$ -axis and points in the direction of the satellite's center of mass, while  $y_F$ -axis completes a right-handed system. The  $R_{BF}$  (*Flight-Body*) matrix gives the transformation between the F-system and the B-system through the attitude angles ( $\phi$ ,  $\theta$ ,  $\psi$ ) varying in time; the

aforementioned known time-dependent terms (one for each attitude angle) are provided by metadata files

$$R_{BF} = \begin{bmatrix} \cos \psi \cos \vartheta & \sin \psi \cos \vartheta + \cos \psi \sin \vartheta \sin \varphi & \sin \psi \sin \vartheta - \cos \psi \cos \vartheta \sin \varphi \\ -\cos \vartheta \sin \psi & \cos \psi \cos \vartheta - \sin \psi \sin \vartheta \sin \varphi & \cos \psi \sin \vartheta + \cos \vartheta \sin \psi \sin \varphi \\ \sin \vartheta & -\cos \vartheta \sin \varphi & \cos \vartheta \cos \varphi \end{bmatrix} \quad (1)$$

- Earth Centered Inertial (ECI) coordinate system (I) - the origin is located at the Earth's center of mass, the X-axis points to the Vernal Equinox relative to a certain epoch (J2000 -1 January 2000, h 12.00), the Z-axis points to the celestial North Pole in the same epoch while the Y-axis completes a right-handed system. The  $R_{FI}$  (*Inertial-Flight*) matrix gives the transformation between the I-system and F-system; it is a function of the Keplerian orbital parameters and thus varies in time within each scene

$$R_{FI} = \begin{bmatrix} -\sin U \cos \Omega - \sin \Omega \cos i \cos U & -\sin \Omega \sin U + \cos U \cos \Omega \cos i & \sin i \cos U \\ -\sin \Omega \sin i & \sin i \cos \Omega & -\cos i \\ \cos \Omega \cos U + \sin \Omega \cos i \sin U & \sin U & -\sin \Omega \cos U - \cos \Omega \cos i \sin U & -\sin i \sin U \end{bmatrix} \quad (2)$$

where  $U = \omega + v$

Finally, it is well known that the transformation between the considered realization of WGS84 and the ECI coordinate system is driven by precession, nutation, polar motion and Earth rotation matrices (Kaula, 1966).

It is now possible to write the collinearity equations in an explicit form for a generic ground point

$$x_s = f \frac{R_1 |X_{tl} - X_{Sl}|}{R_3 |X_{tl} - X_{Sl}|} \quad y_s = f \frac{R_2 |X_{tl} - X_{Sl}|}{R_3 |X_{tl} - X_{Sl}|} \quad (3)$$

where ( $x_s$ ,  $y_s$ ) are the image coordinates,  $f$  is the focal length,  $R_1$ ,  $R_2$ ,  $R_3$  are the rows of the total rotation matrix  $R = R_{SB} R_{BF} R_{FI}$  and ( $X_{tl}$ ,  $X_{Sl}$ ) are the ground point and the satellite positions in ECI system.

With simple geometric considerations (Figure 1) it is possible to write the collinearity equations as functions of the image coordinates (I, J):

$$\frac{x_s}{f} = \text{tg} \beta = \frac{d_{\text{pix}}}{f} [J - \text{int}(J) - J_0] \quad (4)$$

$$\frac{y_s}{f} = -\text{tg} \alpha = -\frac{d_{\text{pix}}}{f} [(I - I_0) + d_1 (I - I_0) + d_2 (I - I_0)^2]$$

where  $d_{\text{pix}}$  is the image pixel dimension, (I-column, J-row) are the image coordinates (in pixels) and ( $I_0$ ,  $J_0$ ) are the principal point coordinates (in pixels). It has to be noted that  $J_0$  may be assumed equal to 0.5 and two self-calibration parameters are included in the second equation (4) only; on the contrary, it is not introduced a third self-calibration parameter  $K$  suited to account for a possible misalignment of the pixel array in the focal plane, affecting the J coordinate, since it is not estimable separately from the sensor attitude parameters.

Substituting equations (4) into equations (3) the collinearity equations become:

$$R_1 |X_{II} - X_{SI}| - \left( \frac{d_{pix}}{f} [J - \text{int}(J) - J_0] \right) R_3 |X_{II} - X_{SI}| = 0$$

$$R_2 |X_{II} - X_{SI}| + \left( \frac{d_{pix}}{f} [(I - I_0) + d_1(I - I_0) + d_2(I - I_0)^2] \right) R_3 |X_{II} - X_{SI}| = 0$$
(5)

these equations are linearized with respect to both the parameters aforementioned and to the image and ground coordinates (Teunissen, 2001).

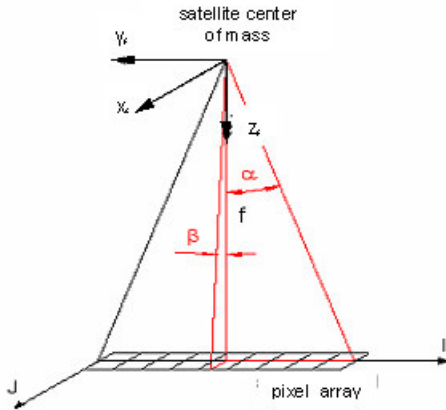


Figure 1. Sensor (S) and image coordinate systems.

## 2.2 Parameter estimation strategy

As regards the full parametrization aforementioned, two major items have to be underlined:

- approximate values for all parameters may be derived from the information contained into the metadata files released together with the imagery or they are simply fixed to zero (2<sup>nd</sup> order polynomial coefficients for attitude angles); nevertheless, it has to be noted that EROS-A metadata are scarce (few state vectors for positions and attitudes along the orbital arc) and may be quite rough (errors up to kilometers for the imagery direct georeferencing) so that a preliminar improvement is generally useful, whilst QuickBird metadata are quite rich (hundreds of state vectors for positions and attitudes along the orbital arc) and accurate (errors within few tens of meters for the imagery direct georeferencing)
- in theory these approximate values must be corrected by an estimation process based on a suitable number of Ground Control Points (GCPs), for which collinearity equations are written; nevertheless, since the orbital arc related to each image acquisition is quite short if compared to a complete satellite revolution around the Earth (some thousandths), some Keplerian parameters are not estimable at all ( $a$ ,  $e$ ,  $\omega$ ) and others (like  $i$ ,  $\Omega$ ,  $T_p$ ) are extremely correlated among them and with sensor attitude and viewing geometry parameters

In order to avoid instability in the estimation process due to high correlations among remaining parameter corrections leading to a pseudo-singularity, Singular Value Decomposition (SVD) is employed to solve the linearized collinearity equations system in the least squares sense (Golub et al., 1993; Strang et al., 1997). As usual, the solution is obtained iteratively due to non linearity; the iterative procedure is stopped when the estimated variance of unit weight  $\hat{\sigma}_0$  reaches a minimum. Before the second iteration, it is evaluated the ground

displacement due to atmospheric refraction at each GCP; GCP coordinates are corrected in order to eliminate the refraction effect; note that atmospheric refraction is relevant under large *off-nadir* acquisition angles (0.5 m at 10°, 7 m at 50°).

SVD strategy allows to single out parameter corrections which are practically undetermined by the observations and need to be constrained to their initial (approximate) values. The threshold used to exclude a parameter correction from the estimation is based on the statistical significance of its impact on the estimated variance of unit weight  $\hat{\sigma}_0$  (Press et al., 1992).

Moreover, the statistical significance of the estimable parameter corrections are checked by a Fisher F-test so to avoid overparametrization; in case of not statistically significant parameter corrections, they are removed and the estimation process is repeated until all corrections are significant.

The formal structure of the functional model with full parametrization for the final estimation is the following

$$A\xi + D\eta + d = 0$$
(6)

where A is the design matrix

$$A = \begin{bmatrix} A_1 \\ A_2 \\ \vdots \\ A_n \end{bmatrix} \quad A_i = \begin{bmatrix} \frac{\partial F_1}{\partial a_0} & \frac{\partial F_1}{\partial a_1} & \frac{\partial F_1}{\partial a_2} & \frac{\partial F_1}{\partial a_0} & \frac{\partial F_1}{\partial a_1} & \frac{\partial F_1}{\partial a_2} & \frac{\partial F_1}{\partial \alpha_0} & \frac{\partial F_1}{\partial \alpha_1} & \frac{\partial F_1}{\partial \alpha_2} & \frac{\partial F_1}{\partial \alpha} & \frac{\partial F_1}{\partial T_p} & \frac{\partial F_1}{\partial i} & \frac{\partial F_1}{\partial i_2} \\ \frac{\partial F_2}{\partial a_0} & \frac{\partial F_2}{\partial a_1} & \frac{\partial F_2}{\partial a_2} & \frac{\partial F_2}{\partial a_0} & \frac{\partial F_2}{\partial a_1} & \frac{\partial F_2}{\partial a_2} & \frac{\partial F_2}{\partial \alpha_0} & \frac{\partial F_2}{\partial \alpha_1} & \frac{\partial F_2}{\partial \alpha_2} & \frac{\partial F_2}{\partial \alpha} & \frac{\partial F_2}{\partial T_p} & \frac{\partial F_2}{\partial i} & \frac{\partial F_2}{\partial i_2} \\ \frac{\partial F_3}{\partial a_0} & \frac{\partial F_3}{\partial a_1} & \frac{\partial F_3}{\partial a_2} & \frac{\partial F_3}{\partial a_0} & \frac{\partial F_3}{\partial a_1} & \frac{\partial F_3}{\partial a_2} & \frac{\partial F_3}{\partial \alpha_0} & \frac{\partial F_3}{\partial \alpha_1} & \frac{\partial F_3}{\partial \alpha_2} & \frac{\partial F_3}{\partial \alpha} & \frac{\partial F_3}{\partial T_p} & \frac{\partial F_3}{\partial i} & \frac{\partial F_3}{\partial i_2} \end{bmatrix}$$
(7)

D is the matrix of observation coefficients

$$D = \begin{bmatrix} D_1 & & 0 \\ & D_2 & \\ & & \ddots \\ 0 & & & D_n \end{bmatrix} \quad D_i = \begin{bmatrix} \frac{\partial F_1}{\partial I} & \frac{\partial F_1}{\partial J} & \frac{\partial F_1}{\partial X_t} & \frac{\partial F_1}{\partial Y_t} & \frac{\partial F_1}{\partial Z_t} \\ \frac{\partial F_2}{\partial I} & \frac{\partial F_2}{\partial J} & \frac{\partial F_2}{\partial X_t} & \frac{\partial F_2}{\partial Y_t} & \frac{\partial F_2}{\partial Z_t} \end{bmatrix}$$
(8)

d is the known term

$$d = \begin{bmatrix} d_1 \\ \vdots \\ d_n \end{bmatrix} \quad d_i = \begin{bmatrix} F_1(\tilde{y}, \tilde{x}) \\ F_2(\tilde{y}, \tilde{x}) \end{bmatrix}$$
(9)

$\xi, \eta$  are the corrections to parameters and to observations (image and GCP coordinates).

As regards the stochastic model, a simple diagonal cofactor matrix for observation ( $I, J; X_t, Y_t, Z_t$ ) is assumed; standard deviations of the image observations are set equal considering that manual collimation tests carried out independently by different operators showed that an accuracy ranging from 1/3 to 1/2 pixel in image coordinates may be routinely achieved; for the GCP coordinates standard deviations are usually set equal to mean values obtained during their direct surveys or cartographic selection.

At the end of the estimation process, the achievable external accuracy is evaluated by the RMSE of the CP coordinate residuals. It is well known that CP are known ground points not used in the parameter estimation process, and it has to be underlined that the atmospheric refraction has to be accounted for in this case too.

## 3. ETH RIGOROUS MODEL (M2)

The second model used in this work is a rigorous sensor model for pushbroom linear array sensors, carried on airborne or spaceborne platforms. It estimates the parameters modelling the sensor internal and external orientation through a bundle adjustment, using a suitable number of ground control points. The sensor position and attitude are modelled by second order

piecewise polynomial functions depending on time. Additionally the polynomial degree can be reduced to get linear functions. Through the self-calibration, the systematic errors due to principal point displacement, focal length variation, radial symmetric and decentering lens distortion, scale variation in CCD line direction and the CCD line rotation in the focal plane are estimated. The choice of the unknown self-calibration parameters to estimate is based on the analysis of the cross-correlation between the self-calibration parameters, the external orientation parameters and the ground coordinates of the TPs. The solution is computed with a least squares method. A blunder detection procedure is integrated for the automatic detection of wrong image coordinate measurement. The adjustment results are analyzed in terms of internal and external accuracy, through the standard deviations of the unknown parameters and the RMSE of the check points. The model have been used for the orientation of different spaceborne linear sensors, like MOMS-02, SPOT-5/HRS, ASTER-VNIR, EROS-A1 and MISR. For more details, see (Poli, 2005).

#### 4. RESULTS

The images were acquired on 1<sup>st</sup> June, 2004 over the village of Augusta (Sicily), in Italy, with viewing angles about +/- 27° and had a mean resolution of about 75 cm.

From the image metadata files the initial approximations from the sensor position and attitude and for the internal orientation (focal length, CCD size) have been extracted.

In addition the images have been oriented using the commercial software OrthoEngine 9.0 (PCI Geomatica). Overall there were available 39 ground points surveyed by GPS with mean horizontal and vertical accuracy of 10 and 20 cm respectively (Figure 2); some tests were performed with different numbers of GCPs and CPs (Figure 3).

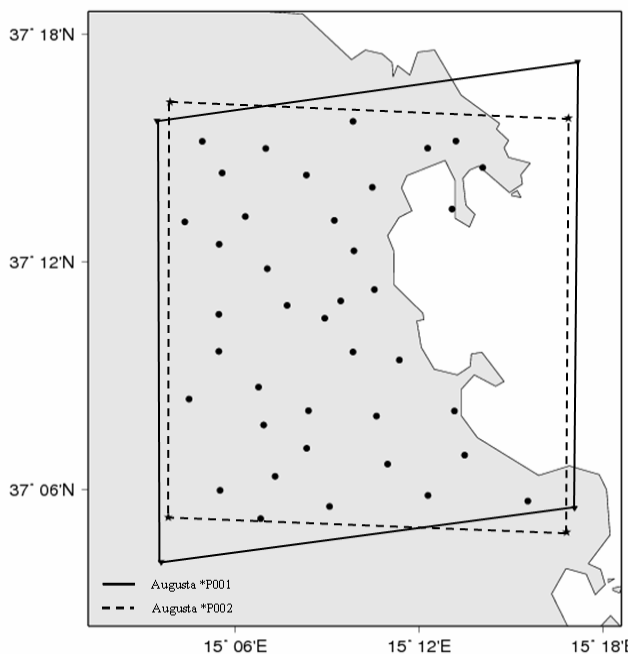


Figure 2. Distribution of the 39 ground points in Augusta region.

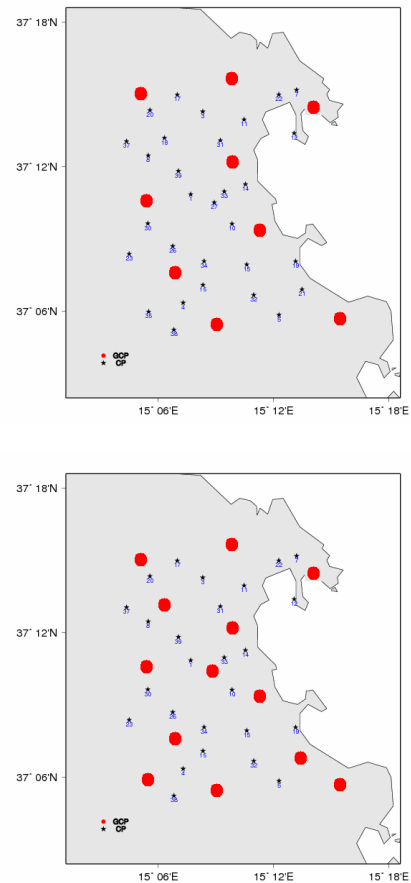


Figure 3. Distribution of 9 (up) and 13 (down) GCPs.

The georeferencing processings included:

- orientation of the single images with rigorous model M1, analysis of the RMSE of the check points in function of the GCPs number and distribution; comparison with OrthoEngine results
- orientation of the stereo pair with rigorous model M2, with analysis of the correlation and significance of the unknown parameters in order to estimate the self-calibration parameters and the polynomial function that best fits with satellite trajectory.

##### 4.1 Georeferencing of Single images

This operation was carried out both by the SISAR software (implementing the rigorous model M1) and the OrthoEngine commercial software.

As regards SISAR solution through SVD, for both image orientations the following parameters were estimated only:  $a_0$ ,  $a_1$ ,  $b_0$ ,  $b_1$ ,  $c_0$ .

No detailed information are available about the model and the strategy solution implemented in OrthoEngine, except for the general description of the Toutin's rigorous model which may be found in (Toutin, 2004) and references therein.

As mentioned before, the RMSE of the CP coordinate residuals was computed to represent the achievable accuracy (Figure 4).

Mean accuracies are similar, around 1.8 pixel for OrthoEngine and 2.0 pixel for SISAR; it has to be noted that for both software these accuracies are already achieved in the test with 13 GCP

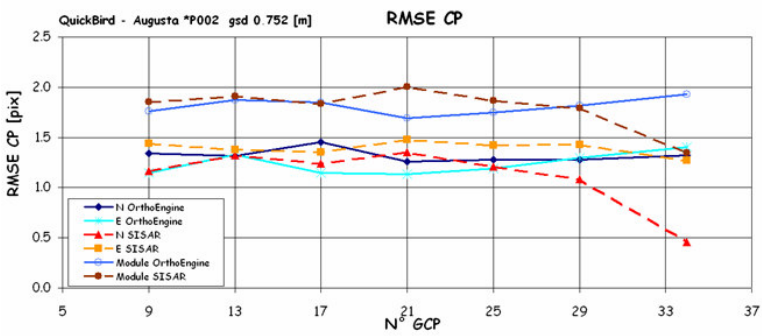
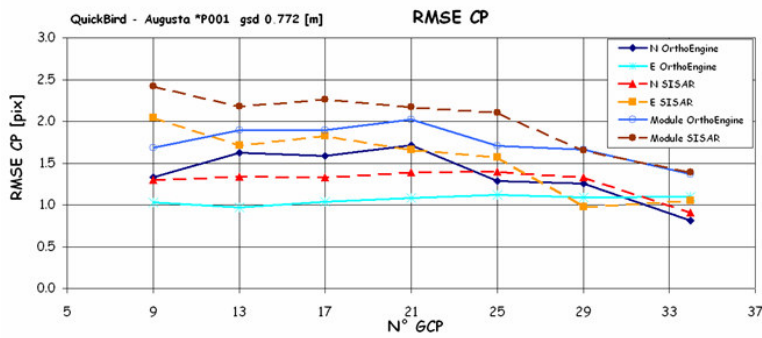


Figure 4. External accuracies vs. GCP number obtained in SISAR for Augusta: image 1 (up), image 2 (down).

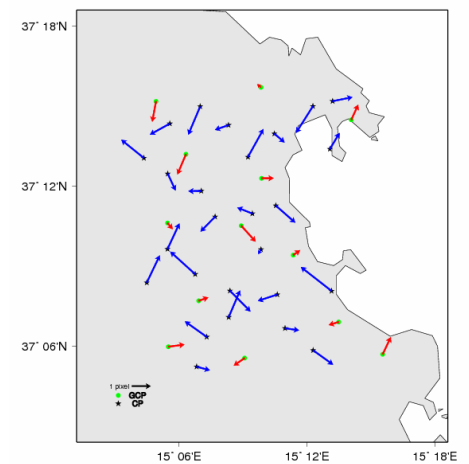
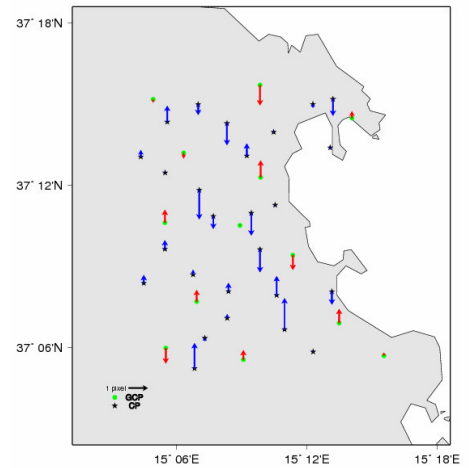


Figure 5. Residuals distribution of GCPs (red segments) and CPs (blue segments) using ETH rigorous model with 13 GCPs. Top: errors in height, Bottom: errors in planimetry

#### 4.2 Georeferencing of Stereo images

For this operation the rigorous model M2 implemented at ETH Zurich was used. New sensors can be easily imported in the software, by creating a file containing the sensor and images characteristics (image size, focal length, viewing angles). This data were available in the metadata files. The pixel size was computed from the geometric relationships between flying height, focal length and ground resolution.

The approximations for the external orientation parameters have been calculated from the ephemeris. The sensor position and attitude (quaternions) provided every 0.20 seconds were interpolated with cubic splines for the time of acquisition of all image lines.

The GCPs distributions shown in Figure 3 was used for these tests too. The software was run with different input settings (number of segments and polynomial degrees for the external orientation modelling). The self-calibration parameters were estimated avoiding any correlation with the external orientation parameters and tie point coordinates.

The most significant results were achieved using quadratic functions for the orientation modelling and 2 segments. Concerning the internal orientation, the self-calibration

parameters that mostly influenced the model were  $k_1$  and  $k_2$  (radial distortion) in both images. By changing the number of GCPs, from a minimum of 9 up to 39, the RMSE in the CPs ranged from 0.8 up to 1.8 pixels (mean GSD 0.75m) for X, Y and Z. In particular, using 13 GCPs the RMSE of the CPs were about 0.80m in planimetry and 0.60m in height (Table 2). The corresponding residuals distribution is shown in figure 5.

RMSE CP	9 GCP			13 GCP		
	N [m]	E [m]	h [m]	N [m]	E [m]	h [m]
	1.22	1.14	1.08	0.92	0.89	0.77

Table 2. RMSE of CPs achieved with ETH model with 9 and 13 GCPs

#### 5. CONCLUSIONS

In this paper the georeferencing of a QuickBird stereopair with rigorous sensor models has been studied. The images have been both oriented separately (2D analysis with SISAR software) and simultaneously (3D analysis with ETH software).

In the orientation of single images with significant off-nadir angle (approx. 27°) accuracy of approximately 1.4 m are achieved with 13 GCPs (surveyed by GPS and manually measured on the images) both by the commercial software OrthoEngine and the original software SISAR.

Concerning the stereo pair orientation with the ETH software, the RMSE in the CPs ranged from 0.8 up to 1.8 pixels (mean GSD 0.75m) for X, Y and Z, depending on the quantity of GCPs. In particular, using 13CPs the RMSE of the CPs were about 0.80m in planimetry and 0.60m in height.

These results can be improved by taking into account the asynchronous acquisition of the sensor. In fact a constant value for the off-nadir viewing angles has been used. In truth, the viewing angle is slightly changing during the image acquisition. If the value of this change is available, it can be included in the model to improve the physical description of the acquisition geometry, as already done for EROS-A1 (Poli, 2005).

Future work include the extension of SISAR software for the simultaneous 3D orientation of stereopairs, not only acquired by QuickBird, but also from other pushbroom sensors with along-track stereo capability.

In addition due to the lack of along-track stereo images from QuickBird, the combination of single images with favourable viewing angle for 3D reconstruction (Kocaman et al., 2006) will be investigated.

#### ACKNOWLEDGMENTS

The authors would like to thank Mr. Fabio Volpe, Eurimage S.p.A. (Rome, Italy), for providing the QuickBird images and Mrs Francesca Fratarcangeli for her valuable collaboration.

This research was partially supported by grants of the Italian Ministry for School, University and Scientific Research (MIUR) in the frame of the project MIUR-COFIN 2005 – "Analisi, comparazione e integrazione di immagini digitali acquisite da piattaforma aerea e satellitare" – National Principal Investigator: S. Dequal (Subproject: "Realization and updating of maps, digital terrain models and geographic databases by high resolution satellite imagery: methodological aspects and relevant applications" – Local Principal Investigator: M. Crespi)

#### REFERENCES

Baiocchi V., Crespi M., De Vendictis L., Giannone F., 2004. A new rigorous model for the orthorectification of synchronous and asynchronous high resolution imagery. Proc. of the 24th EARSeL Symposium, Dubrovnik (Croatia), pp. 461-468

Crespi M., Baiocchi V., De Vendictis L., Lorenzon F., Mezzapesa M. & Tius E., 2003. A new method to orthorectify EROS A1 imagery. Proc. of 2003 Tyrrhenian International Workshop on Remote Sensing, pp. 566-575

Fratarcangeli F., 2006. Ortorettificazione di immagini satellitari ad alta risoluzione acquisite dalla piattaforma QuickBird: sviluppo di un modello rigoroso ed implementazione di un software. Degree thesis in Environmental Engineering (in Italian) Supervisors: M. Crespi, F. Giannone

Golub G. H., Van Loan C. F., 1993. Matrix Computation. The Johns Hopkins University Press, Baltimore and London.

Kaula W. M., 1966. Theory of Satellite Geodesy Blaisdell Publishing Company.

Kocaman S., Zhang, L., Gruen, A., Poli, D., 2006. 3D City Modeling from High-resolution Satellite Images. Published in ISPRS Workshop on Topographic Mapping from Space, 14-16 February 2006, Ankara, Turkey.

Noerdlinger P. D., 1999. Atmospheric refraction effects in Earth remote sensing. ISPRS Journal of Photogrammetry & Remote Sensing, 54 pp. 360–373.

Poli, D., 2005. Modelling of Spaceborne Linear Array Sensors. Diss., Technische Wissenschaften ETH Zurich, Nr. 15894, 2005, IGP Mitteilung N. 85.

Press W. H., Teukolsky S. A., Vetterling W. T., Flannery B. P., 1992. Numerical Recipes in C: The Art of Scientific Computing. Cambridge University Press (ISBN 0-521-43108-5), <http://www.nr.com> (accessed on April 10, 2006).

Strang G., Borre K., 1997. Linear Algebra, Geodesy and GPS, Wellesley-Cambridge Press, Wellesley.

Teunissen P. J. G., 2001. Adjustment theory. Series on Mathematical Geodesy and Positioning, Delft University Press

Toutin T., 2004. Review article: Geometric processing of remote sensing images: models, algorithms and methods, International Journal of Remote Sensing, 25 pp. 1893-1924.

Westin T., 1990. Precision Rectification of SPOT Imagery Photogrammetric Engineering and Remote Sensing, 56 pp. 247-253.